THE JOURNAL OF BIOLOGICAL CHEMISTRY

Vol. 270, No. 26, Issue of June 30, pp. 15515–15522, 1995
*Printed in U.S.A.*

# Purification of the Spliceosome *A*-Complex and Its Visualization by Electron Microscopy*

(Received for publication, March 16, 1995, and in revised form, May 1, 1995)

**Eric Furman and Dohn G. Glitz‡**

*From the Department of Biological Chemistry, UCLA School of Medicine, and the Molecular Biology Institute, University of California, Los Angeles, California 90024-1737*

**Pre-mRNA splicing occurs on spliceosomes, a family of ribonucleoprotein particles. Spliceosome assembly on exogenous adenovirus pre-mRNA was blocked at the *A*-complex (or pre-spliceosome) stage, either by destruction of the small nuclear ribonucleoproteins (snRNPs) that comprise the U4/U5/U6 tri-snRNP complex, or by interference in tri-snRNP assembly and interactions. The *A*-complex was isolated by size exclusion chromatography; homogeneity was shown by electrophoresis in nondenaturing polyacrylamide gels, gradient sedimentation, and electron microscopy. Northern hybridization showed U1 and U2 snRNAs to be present in the preparation, but not U4, U5, or U6. Antibodies specific for a component of the U1 snRNP or for a component that is common to all snRNPs (except U6) each precipitated an *A*-complex containing pre-mRNA, U1 and U2 snRNPs. Electron micrographs showed 230 × 270-Å particles whose two components appear similar to individual U1 and U2 snRNPs. Electron micrographs of an *A*-complex-5′-biotinyl oligonucleotide-streptavidin-gold composite allowed identification of the U2 snRNP within the structure and the localization of the 5′-segment of U2 snRNA at a unique site in the *A*-complex. This region of U2 RNA is adjacent to the developing catalytic center of the spliceosome.**

Eukaryotic mRNA precursors include both the protein-coding information of exons and noncoding intron sequences. Introns are excised by a splicing organelle, the spliceosome, which is made up of small nuclear ribonucleoproteins or snRNPs[1] and several spliceosome-associated proteins (SAPs) (1, 2). Spliceosomes are not simple stable structures, but a dynamic family of particles that assemble on the mRNA precursor and help fold it into a conformation that allows transesterification to proceed (3–6). Various spliceosome forms (*e.g.* *E*-, *A*-, *B*-, *C*-, and *I*-complexes) have been identified by gradient sedimentation (7, 8), electrophoresis (9, 10), gel filtration (11–14), affinity chromatography (15, 16), and genetic means (17–19).

Assembled spliceosomes are less abundant than either their snRNP components or the ribosomes upon which mRNA is translated (20, 21). Both snRNP and SAP composition and conformation change as splicing proceeds, and some SAPs participate only in messenger- or cell-specific splicing (11, 12, 22, 23). Complexes of U1 snRNP and SR proteins have been assembled from purified components (24) but the assembly of spliceosomes from purified components has not yet been possible. It is thus understandable that the physical structure of the spliceosome is not well established. Spliceosomes have been visualized in electron micrographs, but these studies were limited by the small amounts of material, its potential heterogeneity, and the complexity of the purification procedures (14, 25, 26). Detailed analysis of spliceosome structure will require isolation of homogeneous and well-defined forms of the particle as it occurs at specific steps of the splicing cycle.

Specific spliceosome forms can be enriched using complementary oligodeoxynucleotide/RNase H-mediated destruction of selected snRNAs. Alternatively, splicing complexes have been trapped using complementary 2′-*O*-methyl oligoribonucleotides that interfere in spliceosome assembly by blocking RNA-RNA interactions (27–31). In this paper we describe extension of each of these strategies, allowing the isolation of significant amounts of a spliceosomal *A*-complex composed of pre-mRNA, U1 and U2 snRNPs, and probably several SAPs (10, 11, 16). We show electron micrographs of the HeLa cell *A*-complex and, using a 5′-biotinyl-2′-*O*-methyl oligoribonucleotide and a streptavidin-gold marker, we identify the snRNPs within the *A*-complex and localize the 5′ segment of the U2 snRNA and thus the developing center of catalysis in the spliceosome.

## EXPERIMENTAL PROCEDURES

*Oligonucleotides*—A Milligen Cyclone DNA synthesizer was used to prepare both DNA and 2′-*O*-methyl RNA oligomers and in some cases to add a single 5′-biotin through a 9-carbon spacer. β-Cyanoethyl phosphoramidite precursors (32) were purchased from Glen Research, and the Milligen program for RNA synthesis was used in the preparation of 2′-*O*-methyl RNA oligomers. All oligonucleotides were purified by ion exchange HPLC on a Bio-Rad TSK-DEAE-5-PW column (33). The oligonucleotides used in these studies are listed in Table I.

*Splicing Extracts*—HeLa cells were grown to a density of 3–5 × $10^5$ cells/ml and nuclear extracts were prepared as described by Dignam *et al.* (34). Thirty-two liters of HeLa cells typically produced 30 ml of nuclear extract containing 8–12 mg/ml protein. When used as 35% of a splicing reaction mixture this material gave reproducible and efficient splicing. Preparation of ribonuclease H-treated extracts followed Black and Steitz (35). Reaction mixtures (0.8 ml) included 93% nuclear extract, 5 μM cDNA-U4D, 20 μM cDNA-U5E, 25 μM cDNA-U6B, 1.5 mM ATP, 5 mM creatine phosphate, 2 mM $MgCl_2$, and 0.05 unit/μl RNase H (U. S. Biochemical Corp.). Reaction mixtures were incubated at 30 °C for 1 h, followed by the addition of 0.09 unit/μl RNase-free DNase I (Stratagene) and incubation at 30 °C for an additional 15 min. Small aliquots of extracts were flash frozen in liquid nitrogen and stored at −80 °C.

*In Vitro Splicing*—Adenovirus pre-mRNA was transcribed from a plasmid derived from the *Bgl*-cleaved pSPAd construct (36, 37) and supplied to us by Dr. D. Black. The Ambion SP6 *in vitro* transcription kit was used; full-length (417 nucleotide) transcripts were purified by

* This work was supported by National Science Foundation Grant DMB 89–20753, National Institutes of Health Grant GM 51195, and a grant from the UCLA Jonsson Cancer Center Foundation. The costs of publication of this article were defrayed in part by the payment of page charges. This article must therefore be hereby marked "*advertisement*" in accordance with 18 U.S.C. Section 1734 solely to indicate this fact.

‡ To whom correspondence should be addressed: Dept. of Biological Chemistry, UCLA School of Medicine, 10833 LeConte Ave., Los Angeles, CA 90024-1737. Tel.: 310-825-1144; Fax: 310-206-5272; E-mail: DGlitz@Biochem.Medsch.UCLA.edu.

[1] The abbreviations used are: snRNP, small nuclear ribonucleoprotein; snRNA, small nuclear RNA; SAP, spliceosome associated protein; HPLC, high performance liquid chromatography; FPLC, fast protein liquid chromatography; cOmeRNA, complementary 2′-*O*-methyl oligoribonucleotide; cDNA, complementary oligodeoxyribonucleotide.

electrophoresis in a 5% polyacrylamide gel and electroelution. Splicing reactions (25, 100, 300, or 750 μl) were conducted as described by Krainer *et al.* (38), except RNasin and polyvinyl alcohol were omitted and final concentrations of 1.5 mM ATP, 5 mM creatine phosphate, 2 mM $MgCl_2$, 60 mM KCl, and 0.05 μM pre-mRNA were used. Reaction mixtures lacking pre-mRNA were assembled with and without oligonucleotides 5′-biotinyl-cOmeRNA-U2A (8–10 μM), cOmeRNA-U4A (15 μM), and cDNA-U5C (25 μM) and incubated for 15 min at 30 °C; pre-mRNA was then added and incubation was continued for 1 h at 30 °C.

*Electrophoretic Analysis*—Spliceosome complexes were analyzed by fractionation on nondenaturing 4% (80:1) polyacrylamide gels in 75 mM Tris glycine, pH 8.8. Samples (on ice) were adjusted to the same volume and composition by addition of cold H4 buffer (25 mM Tris-HCl, pH 7.8, 60 mM KCl, 2 mM $MgCl_2$, 2 μg/ml aprotinin, and 2 μg/ml leupeptin). Heparin was added to a level of 0.17 mg/ml prior to electrophoresis at room temperature in a Bio-Rad Protean apparatus (30 min at 30 V followed by 1 h at 300 V and 1.5 h at 375 V). Splicing products were analyzed after isolation of the RNA from the splicing reactions (38). Reaction products were fractionated on 10% (19:1) polyacrylamide gels containing 7 M urea in Tris borate-EDTA buffer, pH 8.3. Pre-mRNA, spliced product, exon 1, released intron lariat, and the lariat-exon 2 intermediate are each identified by their mobility (36).

*Isolation of A-Complex*—Splicing reaction mixtures containing trapped *A*-complex (100, 300, or 750 μl) were chilled on ice and 15 μg of carrier yeast RNA was added. Samples were centrifuged for 10 min at 10,000 × *g* and applied to a Pharmacia HR 10/30 Superose 6 FPLC column that had been equilibrated with ice-cold H4 buffer and adapted for use with a Waters HPLC system. A flow rate of 0.3 ml/min was maintained until the first (void volume) peak had been collected, at which point the rate was increased to 0.6 ml/min. In most instances the first 0.4 ml of the void volume peak from 100 μl of reaction mixtures was used for electron microscopy.

The first fraction (1.2 ml) of the Superose 6 void volume peak from 0.75-ml splicing reaction mixtures was sometimes subjected to sucrose density gradient sedimentation. Samples were loaded on 37-ml 10–40% gradients prepared in H4 buffer and centrifuged for 15 h at 20,000 rpm in a Spinco SW28 rotor. Fractions corresponding to sedimentation values of about 40–50 S were found to contain *A*-complex.

*Northern Hybridizations*—RNA was isolated by phenol-chloroform extraction and fractionated on a 10% (19:1) polyacrylamide gel containing 7 M urea. The RNA was transferred electrophoretically to a GT nylon membrane (Bio-Rad) using 1 × hydrolink (J. T. Baker) buffer. Oligodeoxynucleotide probes were labeled with polynucleotide kinase (Pharmacia) and [$^{32}$P]ATP (DuPont NEN) at a specific activity of 1–3 mCi/μmol. Hybridizations were carried out overnight at 37 °C according to the Bio-Rad protocol, and the blots were then washed three times with 6 × SSC (0.9 M NaCl, 0.09 M sodium citrate, pH 7.0) plus 0.2% SDS at 23 °C for 30 min (each) followed by one wash at 37 °C for 10 min in the same solution.

*Immunoprecipitation*—Anti-endoplasmic reticulum membrane protein 13D6/G8 (39) and anti-U1 70K protein (40) monoclonal antibodies were obtained as tissue culture supernatants from Dr. David Meyer and Dr. Sallie Hoch, respectively. Dr. E. DeRobertis contributed the anti-SM antibody (41). Antibodies in 1.5 M glycine plus 3 M NaCl, pH 8.9, were immobilized on Ultralink Protein A Plus beads (Pierce) by rocking on a nutator at 23 °C for 1 h and washed with 20 bead volumes of 50 mM Tris-HCl, pH 8.0, plus 150 mM KCl. To block nonspecific sites, rocking was continued for 16 h at 4 °C in 50 mM Tris-HCl, pH 7.7, 150 mM KCl, 2 mM $MgCl_2$, 0.05% Nonidet P-40, 20 mg/ml acetylated bovine serum albumin, and 0.1 mg/ml yeast tRNA. The beads were then washed with a total of 20 bead volumes of IP buffer (50 mM Tris, pH 7.7, 150 mM KCl, 2 mM $MgCl_2$, 0.05% Nonidet P-40, 0.1 mg/ml acetylated bovine serum albumin, 0.1 mg/ml yeast RNA, and 0.05 mM dithiothreitol). A 300-μl splicing reaction containing RNase H-treated nuclear extract was fractionated by Superose 6 chromatography and the early fraction (1 ml) was collected, adjusted to the IP buffer conditions, and divided into four aliquots (500 μl: about 0.06 $A_{280}$/each). Each aliquot was added to 50 μl of immobilized antibodies, rocked at 4 °C for 2 h, and then washed with 40 bead volumes of IP buffer. Bound RNAs were recovered from the support by proteinase K digestion.

*Electron Microscopy*—Samples were adsorbed to thin carbon support films, negatively contrasted using a double carbon technique (42), and examined at 80,000 × magnification using a JEOL 1200EX electron microscope operated at 80 kV. Computer-generated images were produced by scanning individual particles with a Macintosh scanner and Quadra computer with the OFOTO program. Contrast was enhanced using Adobe Photoshop software, and images were printed at 300 dpi.

*Localization of 5′-Biotinyl-cOmeRNA-U2A*—Splicing reactions (100 μl) containing RNase H-treated nuclear extract were incubated with 8–10 μM 5′-biotinyl-cOmeRNA-U2A for 15 min at 30 °C; pre-mRNA was then added and incubation was continued for 1 h. After Superose 6 chromatography, streptavidin-gold (5 nm, EY Laboratories) was added to the early fraction of the void volume peak at a final concentration of 2 μM. Samples were incubated for 1.5 h on ice and then prepared for electron microscopy as above.

TABLE I
*Oligonucleotides used in these experiments*

| Designation | Sequence | Complementary to nucleotides |
|---|---|---|
| cDNA-U1A | CCACCTTCGTGATCAT | 26–41 of U1 snRNA |
| U2A | AAAAGGCCGAGAAGCGAT | 1–18 of U2 snRNA |
| U2B | AACAGATACTACACTTG | 28–44 of U2 snRNA |
| U4A | GATACTGCCACTGCGCAAAGCT | 1–22 of U4 snRNA |
| U4D | CGGGGTATTGGGAAAAGTTT | 66–85 of U4 snRNA |
| U5C | CTTTAGTAAAAGGCGAAAG | 32–50 of U5 snRNA |
| U5E | TTAAGACTCAGAGTTGTTCC | 64–83 of U5 snRNA |
| U6B | GAACGCTTCACGAATTTGCGT | 75–98 of U6 snRNA |
| cOmeRNA-U2A | CCAAAAGGCCGAGAAGCGAU | 1–20 of U2 snRNA |
| U4A | GAUACUGCCACUGCGCAAAGCU | 1–22 of U4 snRNA |

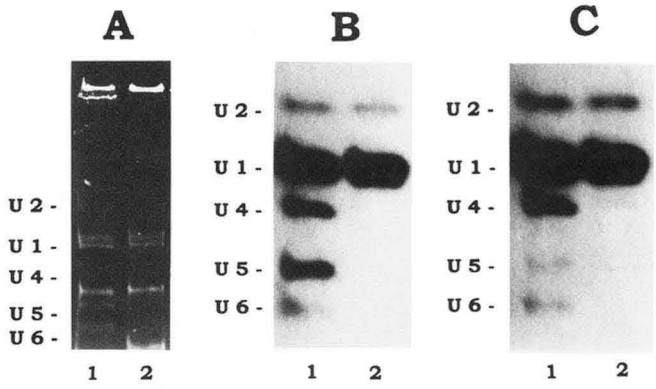


FIG. 1. **Destruction of U4/U6 and U5 snRNP particles with complementary oligodeoxynucleotides and RNase H.** *A*, HeLa cell nuclear extract was treated with 50 units/ml RNase H under splicing conditions for 1 h at 37 °C in the absence (*lane 1*) or presence (*lane 2*) of 5 μM cDNA-U4D, 20 μM cDNA-U5E, and 25 μM cDNA-U6B. The RNA was isolated and fractionated on a 10% denaturing polyacrylamide gel and stained using ethidium bromide. *B*, RNA from the gel in *A* was transferred to a nylon membrane and probed with a mixture of $^{32}$P-labeled cDNAs U1A, U2A, U4D, U5E, and U6B. *C*, the membrane in *B* was stripped and reprobed with $^{32}$P-labeled cDNAs U1A, U2B, U4A, U5C, and U6B.

## RESULTS

*A-Complex Formation: RNase H Destruction of the Tri-snRNP*—One way to halt spliceosome assembly at a specific stage is to destroy a component that is required later in the process (35, 43, 44). We have used RNase H treatment in conjunction with oligodeoxynucleotides that complement segments of U4, U5, and U6 snRNAs to destroy the tri-snRNP complex and cause the accumulation of *A*-complex. Oligonucleotides used in this work are listed in Table I.

Nuclear extracts were supplemented with cDNAs U4D, U5E, and U6B and incubated with RNase H. Fig. 1 illustrates electrophoretic analysis of the result; snRNAs U4, U5, and U6 were present in control nuclear extracts but were undetectable in treated preparations whether in stained gels (Fig. 1*A*) or if probed by Northern analysis using two different sets of complementary oligonucleotides (Fig. 1, *B* and *C*). Much longer exposure of these blots still did not reveal snRNAs U4, U5, and U6.

Treated preparations were examined for the ability to assemble splicing complexes and catalyze splicing. Control nuclear extracts sometimes included cOmeRNA-U2A or a 5′-biotinyl form of this oligoribonucleotide, both of which have been shown to trap the *A*-complex (16, 27, 30). Control and treated extracts

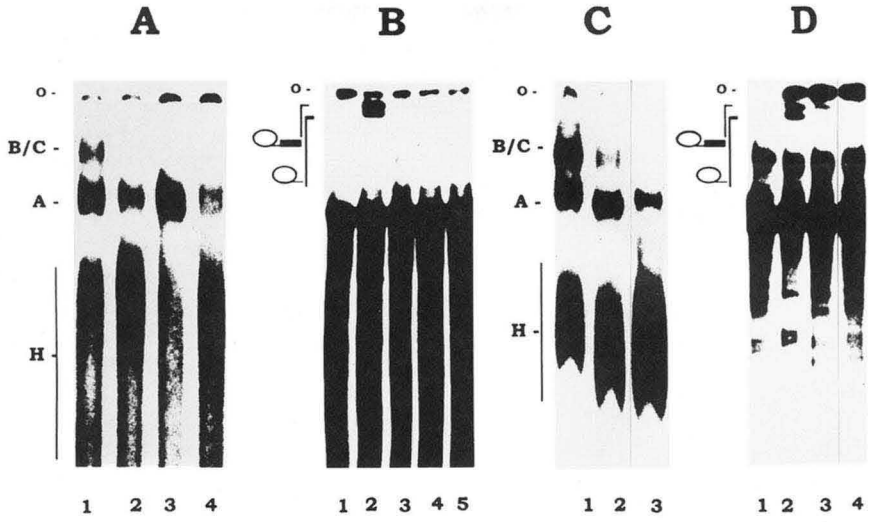


FIG. 2. **Splicing reaction mixtures treated with RNase H in the presence of complementary oligodeoxynucleotides or assembled with complementary 2′-*O*-methyl oligonucleotides efficiently trap spliceosomal *A*-complex.** *A*, splicing reactions containing mock-treated nuclear extract (*lanes 1* and *2*) or nuclear extract that had been treated with RNase H in the presence of cDNAs U4D, U5E, and U6B (*lanes 3* and *4*) were carried out in the presence (*lanes 2* and *4*) or absence (*lanes 1* and *3*) of cOmeRNA-U2A. A 10-μl portion of each reaction was brought to 0.17 mg/ml heparin, and spliceosome complexes were fractionated on a 4% (80:1) nondenaturing polyacrylamide gel. *B*, RNA isolated from 10-μl portions of each reaction above was fractionated on a 10% denaturing polyacrylamide gel. *Lane 1* contained the input pre-mRNA; splicing reactions were run in the presence of cOmeRNA-U2A (*lanes 3* and *5*) and in its absence (*lanes 2* and *4*). Splicing by mock-treated nuclear extract (*lanes 2* and *3*) is compared to nuclear extract treated with RNase H/cDNAs U4D, U5E, and U6B (*lanes 4* and *5*). *C*, splicing reactions containing nuclear extract that was untreated (*lane 1*), included 25 μM cDNA-U5C (*lane 2*), or included cDNA-U5C (25 μM), 5′-biotinyl cOmeRNA-U2A (10 μM), and cOmeRNA-U4A (15 μM) (*lane 3*) were fractionated as in *A* above. *D*, RNA products from 10 μl of the splicing reactions in *C* were fractionated on 10% denaturing polyacrylamide gels. *Lane 1* contained the input pre-mRNA and *lane 2* shows the lariat intermediate and lariat products that accumulate in the absence of blocking oligonucleotides. Products of the reaction that included cDNA-U5C and that containing all three oligonucleotides are shown in *lanes 3* and *4*, respectively.

were incubated with $^{32}$P-labeled adenovirus pre-mRNA under splicing conditions. Portions of each reaction mixture were brought to 0.17 mg/ml heparin (to minimize dissociation of higher molecular weight complexes (30)) and fractionated by electrophoresis on nondenaturing 4% polyacrylamide gels (native gels); Fig. 2*A* shows that both the preparation treated with RNase H/cDNA and that trapped with cOmeRNA-U2A accumulate *A*-complex but, unlike the unblocked control, little or no *B*- or *C*-complex is apparent. RNA from each reaction was isolated and fractionated by electrophoresis on 10% denaturing polyacrylamide gels. The intentionally overexposed gel in Fig. 2*B* shows no evidence of the lariat intermediate or the excised lariat in either the RNase H/cDNA-treated preparation or the cOmeRNA-U2A-trapped extract, confirming that the formation of the *B*-, *C*-, and *I*-complexes is fully blocked in these extracts. The untreated extract, however, shows appreciable quantities of the lariat intermediate and excised lariat.

*A-Complex Formation: Disabling the Tri-snRNP with 2′-O-Methyl Oligoribonucleotides*—A second approach to the isolation of a homogeneous spliceosome population uses complementary 2′-*O*-methyl oligoribonucleotides to block RNA-RNA interactions that are necessary at a specific assembly step and thus trap a defined intermediate form of the complex (16, 27, 29, 30). Although the cOmeRNA-U2A oligomer or its 5′-biotinyl equivalent traps the *A*-complex efficiently, subsequent attempts to purify the *A*-complex showed U4/U5/U6 tri-snRNP contamination. To alleviate this problem we investigated *A*-complex trapping using cOmeRNA-U4A to destabilize the U4/U6 snRNP (16, 29) and cDNA-U5C, which should block an interaction of stem/loop 1 of U5 snRNA with exons 1 and 2 of the pre-mRNA that is necessary for *B*- and *C*-complex formation. DNA/RNA hybrids involving this segment of U5 snRNA are not susceptible to RNase H degradation (44).

Splicing reactions were conducted with nuclear extract that had been supplemented with cDNA-U5C alone or with cDNA-U5C, 5′-biotinyl-cOmeRNA-U2A, and cOmeRNA-U4A together as a "triple trap." Spliceosome complex formation was evaluated by electrophoresis in nondenaturing gels (Fig. 2*C*) and the effectiveness of the traps was assessed by the amounts of lariat intermediate and excised lariat that could be detected in denaturing gels (Fig. 2*D*). It is clear that cDNA-U5C alone is unable to fully block the formation of *B*- and *C*-complexes, while the triple trap results in the accumulation of *A*-complex while allowing no detectable formation of *B*- or *C*-complexes and no accumulation of lariat forms. Addition of cOmeRNA-U4A alone also resulted in *A*-complex accumulation, and allowed formation of only small amounts of lariat products.

*A-Complex Isolation*—Purification of the *A*-complex was based on the absence of other particles of similar size in RNase H-treated and triple trap-blocked trapped splicing extracts. Reaction mixtures of 100, 300, or 750 μl were fractionated on a Superose 6 (HR 10/30) FPLC column adapted for a Waters HPLC system; *A*-complex eluted in the void volume peak with the bulk of the radiolabeled RNA, while significant amounts of protein and nucleic acid were retarded (Fig. 3*A*). The void volume peaks were collected as three fractions: early, middle, and late. Fig. 3*B* shows an electron micrograph of the early fraction from a 100-μl RNase H-treated preparation; a nearly homogeneous population of bipartite particles is seen.

To further verify the identity of the preparation as *A*-complex, early fractions from Superose 6 chromatography of 750-μl reaction mixtures of both RNase H-treated and triple trap blocked preparations were centrifuged through sucrose density gradients. In each case electron micrographs of material in fractions sedimenting at 40–50 S showed homogeneous populations of bipartite particles that were indistinguishable from those seen in the small scale preparations described above. Sample micrographs are shown in Fig. 4. Nondenaturing gel analysis and Northern hybridization showed that the 40–50 S sucrose fraction from the RNase H-treated preparation contained *A*-complex but no *B*/*C*- or *E*/*H*-complex, and confirmed the presence of U1 and U2 snRNAs.

*The A-Complex Is Composed of U1 and U2 snRNPs Bound to Pre-mRNA*—Portions of the early, middle, and late fractions of the void volume peak were analyzed by nondenaturing gel electrophoresis (Fig. 5*A*). It is clear that the early fraction of the peak from the RNase H-treated preparation is highly enriched for *A*-complex. The triple trap blocking strategy appears somewhat less efficient, but some or all of the *E*/*H*-complex in the latter case may result from the destabilization of *A*-complex by cOmeRNA-U2A; several SAPs that interact with the targetted segment of U2 snRNA are thought to stabilize the interaction of pre-mRNA with the U2 snRNP (45–47). In addition, the binding of [$^{32}$P]cOmeRNA-U2A to the *A*-complex in 100-$\mu$l assembly reactions was roughly quantitative when measured after Superose 6 chromatography, but after nondenaturing polyacrylamide gel electrophoresis its binding was markedly reduced.

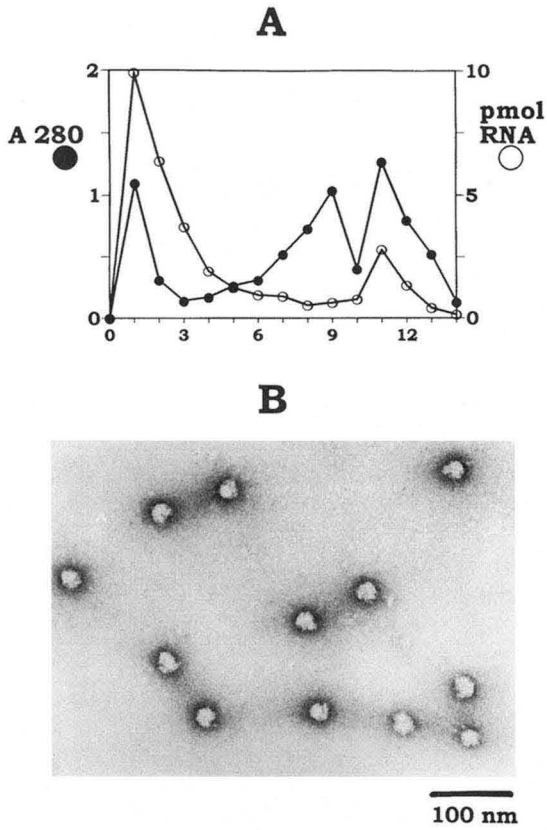


FIG. 3. **Superose 6 chromatography of trapped splicing reactions allows isolation of a homogeneous bipartite particle.** *A*, a 750-$\mu$l splicing reaction containing nuclear extract that had been treated with RNase H and cDNAs U4D, U5E, and U6B was fractionated on a Superose 6 column and 1.2-ml fractions were collected starting with the appearance of the void volume peak. RNA in each fraction was quantitated by relating the amount of $^{32}$P in an aliquot of each fraction to the specific activity of the input pre-mRNA. *B*, a 100-$\mu$l splicing reaction like that in *A* was fractionated as above except that the first 1.2 ml of the void volume peak was collected in three 400-$\mu$l fractions designated early middle and late. Material from the early fraction was adsorbed to a carbon support film and negatively contrasted in order to obtain the electron micrograph. ●, $A_{280}$; ○, pmol of pre-mRNA.

Previous preparations of the *A*-complex were formed on incomplete pre-mRNAs lacking functional 5′ or 3′ splice sites or used a temporal trap, and it is unclear that U1 and U2 snRNPs were simultaneously bound to the pre-mRNA (11–13, 47), the *A*-complex predicted by affinity chromatography (16). A 300-$\mu$l splicing reaction using cDNA/RNase H-treated nuclear extract was chromatographed on Superose 6 and equal portions of the early fraction were immunoprecipitated. The antibodies used were: anti-U1 (70-kDa), a monoclonal antibody to the 70-kDa protein of U1 snRNP (40); anti-SM, a human polyclonal antibody that recognizes the core proteins that comprise the SM domain of the U1, U2, U4, and U5 snRNPs (41, 48); and an antibody to an endoplasmic reticulum membrane protein, used as a control. After immunoprecipitation, the bound RNAs were isolated and fractionated on a 10% denaturing polyacrylamide gel and subsequently transferred to a nylon membrane. An autoradiograph of the membrane prior to Northern hybridization showed radiolabeled pre-mRNA in the anti-U1 (70-kDa) and anti-SM immunoprecipitates, but not the control. Exposures of the same membrane are shown after successive Northern hybridizations with radiolabeled cDNA-U1A (Fig. 5*B*) and a mixture of labeled cDNAs U2B, U4D, U5E, and U6B (Fig. 5*C*). The presence of pre-mRNA, U1 and U2 snRNAs, but not U4, U5, or U6 snRNAs, is apparent prior to immunoprecipitation (Fig. 5, *B* and *C, lanes 5*). More important, the presence of these three components in the sample immunopreciptated with anti-U1 (70-kDa) antibodies (Fig. 5, *B* and *C, lanes 3*) indicates that the *A*-complex in our preparation is composed of U1 and U2 snRNPs bound to the pre-mRNA.

*Electron Microscopy of the A-Complex*—Electron micrographs of the *A*-complex show bipartite particles in a limited number of orientations, as illustrated in the gallery of Fig. 6. In the "double carbon" or "sandwich" technique we used the sam-

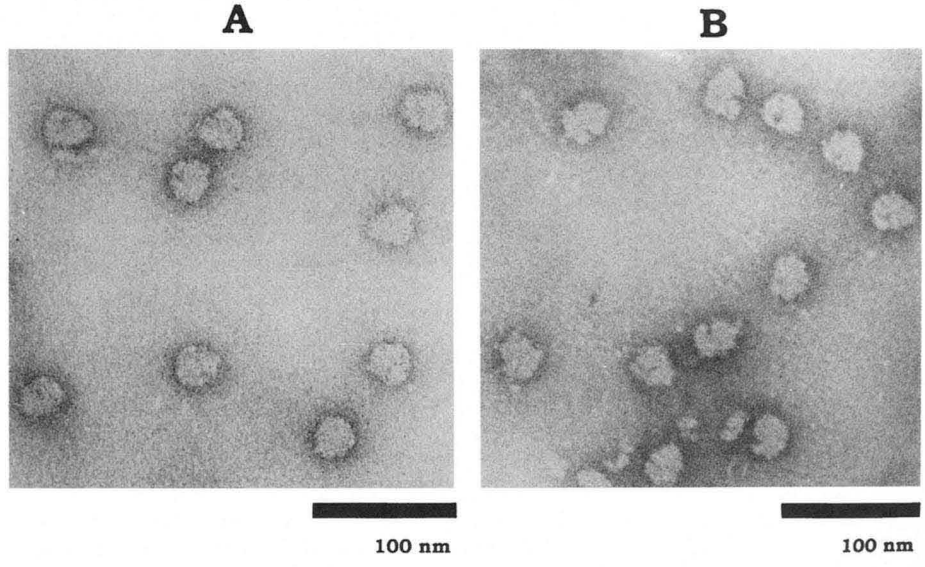


FIG. 4. **Sucrose density gradient sedimentation of the *A*-complex.** Splicing reactions (750 $\mu$l) were fractionated on Superose 6, and the first 1.2 ml of each void volume peak was then fractionated on a 37-ml sucrose density gradient (10–40%). Fractions sedimenting at about 40–50 S were prepared for electron microscopy. *A*, a field from a reaction mixture in which the nuclear extract was treated with RNase H and cDNAs U4D, U5E, and U6B. *B*, a field from a reaction mixture which included cDNA-U5C and cOmeRNAs-U2A and -U4A.

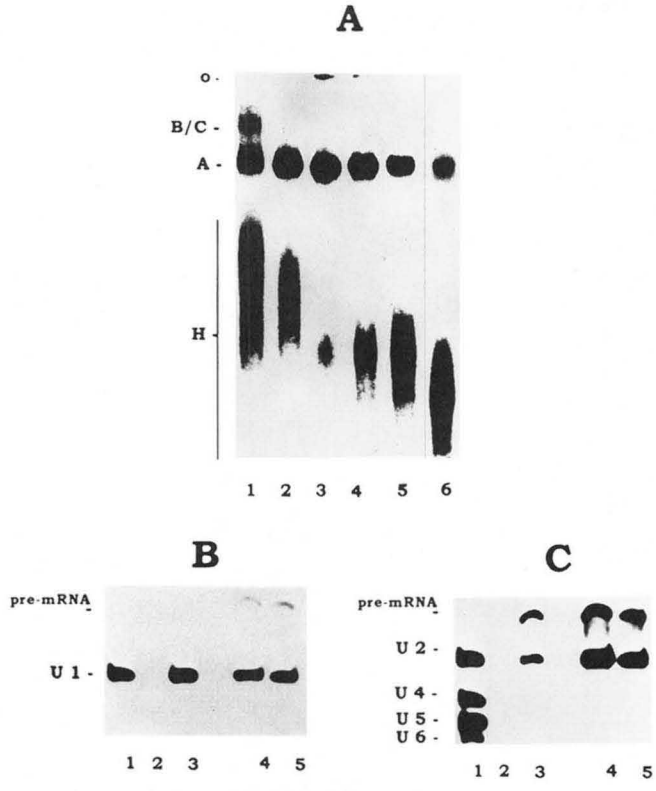


FIG. 5. **The bipartite *A*-complex is composed of U1 and U2 snRNPs bound to the pre-mRNA.** *A*, spliceosome complexes were purified by Superose 6 chromatography and analyzed by nondenaturing polyacrylamide gel electrophoresis. *Lane 1* shows a reaction prepared with untreated nuclear extract, while the nuclear extract for *lane 2* was treated with RNase H and cDNAs U4D, U5E, and U6B. A 750-$\mu$l splicing reaction containing RNase H/cDNA-treated nuclear extract was fractionated on Superose 6; *lanes 3–5* show material from the early, middle, and late portions of the void volume peak, respectively. *Lane 6* shows the composition of the early fraction from chromatography of a splicing reaction that used untreated nuclear extract plus cDNA-U5C, 5′-biotinyl-cOmeRNA-U2A, and cOmeRNA-U4A. *B*, analysis of RNA isolated from immunoprecipitates of the early fraction from chromatography of a 300-$\mu$l splicing reaction prepared with RNase H-treated nuclear extract. RNA was fractionated on a 10% denaturing polyacrylamide gel, transferred to a nylon membrane, and probed with the $^{32}$P-labeled cDNA-U1A. *Lane 1* shows RNAs isolated from 2 $\mu$l of untreated nuclear extract and *lane 5* contained the RNAs from 0.02 $A_{280}$ of the early fraction prior to immunoprecipitation. Antibodies used were: anti-endoplasmic reticulum membrane protein (*lane 2*, control), anti-U1 (70-kDa) (*lane 3*), and anti-SM (*lane 4*). *C*, the membrane in *B* was stripped and reprobed with a mixture of $^{32}$P-labeled cDNAs U2B, U4D, U5E, and U6B.

ple lies between two carbon films; the particles measure about 230 × 270 Å, and they are seen in a limited number of projections. In the most common view, a line of stain separates the ovoid particle into two sections, one of which is slightly smaller than the other. We have arbitrarily arranged the Figure to show the stain line horizontally, with the smaller segment of the particle to the top. The relative size of the two sections shows some variation; we interpret this as due to limited rotation of the particle about its horizontal axis. The separation between the two sections is also somewhat variable, sometimes resulting in the appearance of a small cavity near one end of the stain line or a larger separation of the two components at one end of the horizontal line. The particles also appear in two views that are mirror images of one another; these can arise if one region of the *A*-complex is preferentially adsorbed to the carbon surface and the carbon is folded over itself to trap the particles in the carbon sandwich. These enantiomorphic views are most easily seen in comparison of the images in *columns A* and *B* of *rows 3* and *4* in Fig. 6.

Work with ribosomes has shown that antibodies can serve as topographical markers to localize modified oligodeoxynucleotides that have been hybridized with specific segments of rRNA in the ribosome (*e.g.* Ref. 49). We have used streptavidin-gold as an easily visualized but less precise marker to place 5′-biotinyl-cOmeRNA-U2A, forms of which have been well characterized in their interaction with spliceosomes (16, 27, 30). Splicing reactions (100 $\mu$l) containing cDNA/RNase H-treated nuclear extract were supplemented with 8–10 $\mu$M 5′-biotinyl-cOmeRNA-U2A or 8–10 $\mu$M radiolabeled cOmeRNA-U2A. After Superose 6 chromatography the early fraction of each void volume peak was collected. Radiolabeled oligonucleotide concentration in the early fraction was 5 $\mu$M. In order to limit manipulation and nonspecifc complex formation, streptavidin-gold (5 nm) was added to the 5′-biotinyl-cOmeRNA-U2A fraction to a final level of 2 $\mu$M and after 1.5 h on ice the samples were prepared for electron microscopy. Five independent experiments were conducted and a total of 266 apparent spliceosome-streptavidin-gold complexes were identified and scored; examples are shown in Fig. 7. The predominant site of streptavidin-gold binding (231 complexes) was at the head and neck region of the upper member of the complex, thus identifying this region as the 5′-end of U2 snRNA. Control experiments in which the biotinyl-oligonucleotide was replaced by its unmodified equivalent showed fewer than 10 apparent complexes, and the few instances in which a gold-labeled particle appeared to be associated with a spliceosome showed no preference for any specific site.

## DISCUSSION

In attempts to isolate and structurally analyze the spliceosome *A*-complex we have adapted two previous analytical approaches and one preparative method, modifying and combining them to permit the rapid purification of significant amounts of homogeneous material. The trapping of *A*-complex by destruction of the tri-snRNP particle using a complementary oligodeoxynucleotide and RNase H treatment has been demonstrated qualitatively (43, 44). Here several cDNAs were used to destabilize all three components of the tri-snRNP, and the procedure was scaled up to a preparative level. Alternatively, complementary 2′-*O*-methyl oligoribonucleotides that block specific steps in spliceosome assembly (but do not destroy the snRNPs) have been used to analyze the splicing pathway (16, 27, 28, 30, 31). In this work the approach was scaled up to an appropriate preparative level and multiple blocks were employed so as to maximize the effectiveness of the trapping procedure. Gel chromatography, previously employed in the isolation of spliceosomes, was adapted to allow elution of *A*-complex within 25 min rather than the 20–30 h of Reed *et al.* (14). The combination of effective traps and rapid chromatographic separation results in isolation of a nearly homogeneous preparation of *A*-complex from small scale (100 $\mu$l) reactions. Rapid isolation was considered important, since we hoped to avoid the use of cross-linking reagents. Larger scale preparations (750 $\mu$l) can be further purified by gradient density sedimentation, although there appears to be considerable dissociation of the *A*-complex during this procedure.

Both approaches above allow isolation of homogeneous *A*-complex, but it appears from the nondenaturing gels of Fig. 2*A* that the cDNA/RNase H method results in more efficient recovery and better yields. This may result from the destabilization of the interaction of pre-mRNA and U2 snRNP by cOmeRNA-U2A (45–47), a conclusion that is reinforced by our observation that native gel electrophoresis of the purified material reveals partial dissociation of [$^{32}$P]cOmeRNA-U2A from the *A*-complex. Although the binding of isolated 17 S U2 snRNP

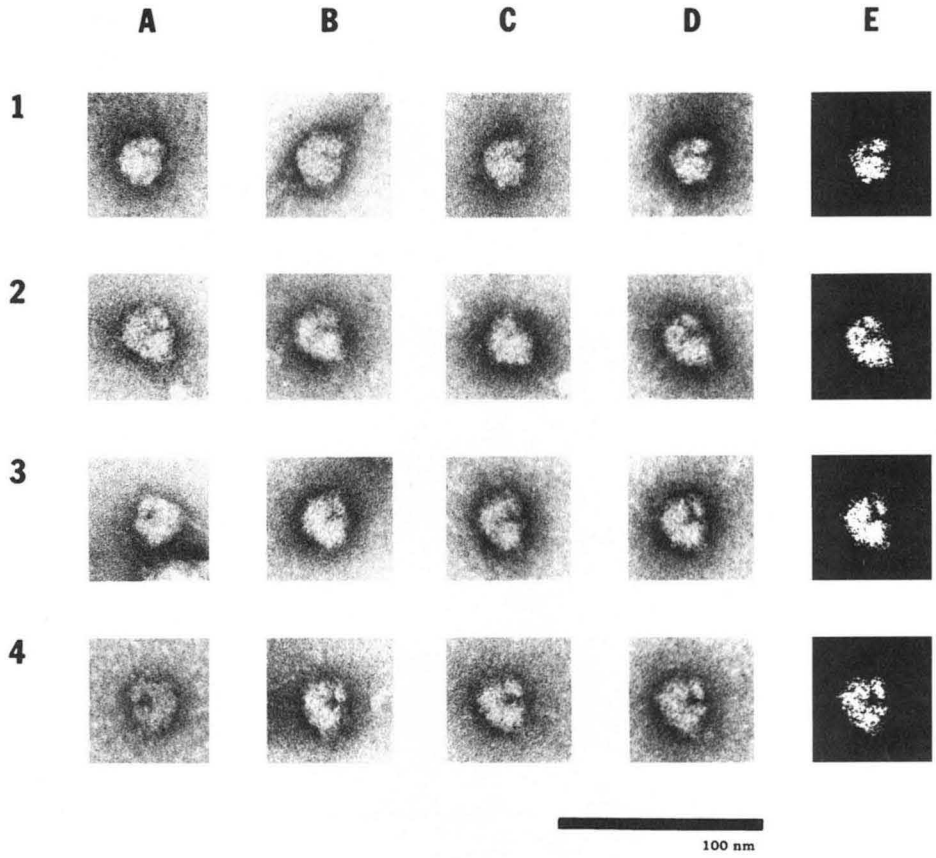


FIG. 6. **A gallery of electron micrographs of the spliceosomal *A*-complex.** *Rows 1–4* show slightly different orientations of the bipartite *A*-complex in which the separation between segments becomes slightly more apparent. *Panels A3* and *A4* show particles oriented to appear as mirror images of the other particles in the row. *Column E* shows computer generated enhancements of the corresponding images in *column D*.

by cOmeRNA-U2A does not disrupt the U2 snRNP, as determined by nondenaturing gel electrophoresis (50), it is likely that the oligoribonucleotide perturbs proteins associated with the 5′-end of U2 snRNA to promote U2 snRNP dissociation from pre-mRNA under conditions used for electrophoresis. Nevertheless, it is clear that by the criteria used here the product isolated by the triple trap blocking approach is indistinguishable from that prepared by cDNA/RNase H treatment. This suggests that the general approach of oligonucleotide blocking could be applied to the isolation and characterization of additional forms of the spliceosome. Electrophoretic analysis of the early fraction of either preparation indicates that the radiolabeled pre-mRNA is predominantly associated with the *A*-complex, electron microscopy shows a homogeneous preparation of particles, and Northern analysis and immunoprecipitation establish that the *A*-complex isolated by our methods is composed of both U1 and U2 snRNPs attached to the pre-mRNA. Furthermore, co-immunoprecipitation shows that the 70-kDa protein and the core proteins that comprise the SM domain are intact. Several SAPs are also expected to be present in these particles, but we have not yet attempted to either demonstrate their presence or to identify them.

Other workers have attempted to visualize the spliceosome. The micrographs of HeLa cell spliceosomes of Reed *et al.* (14) were made by metal shadowing of particles that appear to be of different size and complexity. They used nuclear extract that was enriched for *C*-complex by heating to inactivate a component that is needed for 3′ cleavage and exon linkage, but later work from the Reed laboratory (12) indicates that this trap is variable and that the composition of the *C*-complex differs from that reported earlier. It is therefore reasonable that several of the particles in their micrographs appear to include only two components and, given the differences between shadowing and negative staining, that their size and shape are consistent with the *A*-complex we see. Sibbald *et al.* (26) have visualized HeLa cell splicing complexes by dark field scanning transmission electron microscopy. Their micrographs show three classes of complexes plus mRNA, identified by tagging biotinylated messenger with streptavidin-20 nm gold complexes. Although their technique is quite different and the gold particle is similar in size to the spliceosomes they see, some of their particles could also be equivalent to the *A*-complex seen here. Yeast spliceosomes have also been visualized (25), in this case by negative staining. Detailed characterization was limited by the very small amounts of material that could be isolated; the authors estimated the recovery of 0.1 fmol of spliceosomes from a 200-$\mu$l reaction mixture, insufficient for the generation of micrographs showing many well defined particles. In addition, electron microscopy of yeast and HeLa cell snRNPs has shown significant differences (51), and it may be unrealistic to expect their spliceosomes to be identical in appearance. It is therefore not troubling that our *A*-complex micrographs do not appear to correspond to any of the ovoid particles shown by Clark *et al.* (25).

Individual purified snRNPs have been carefully characterized in the Lührmann (48, 51–52) laboratory. Their micrographs show U1 snRNP as a roughly round body with two unequal protuberances, giving it a somewhat fish-like profile (48, 51–53). The core proteins that assemble with the SM domain have been localized to the main body of the U1 particle (53). The 17 S U2 snRNP includes two globular segments. One part, the body, is present in the 12 S U2 snRNP; it includes the SM domain, the core proteins B′, B, D1, D2, D3, E, F, and G, and the U2-specific proteins A′ and B″. The other segment, the head, contains nine SAP proteins that are thought to be associated with the 5′-end of the U2 snRNA (45). The two domains are separated from one another by an RNase-sensitive thin filament or neck, giving the 17 S U2 snRNP a "dumbell" shape.

The characteristic profiles of the U1 and U2 snRNPs are discernable in our micrographs of *A*-complex in the gallery of Fig. 6. We show the particles oriented so that the U2 snRNP

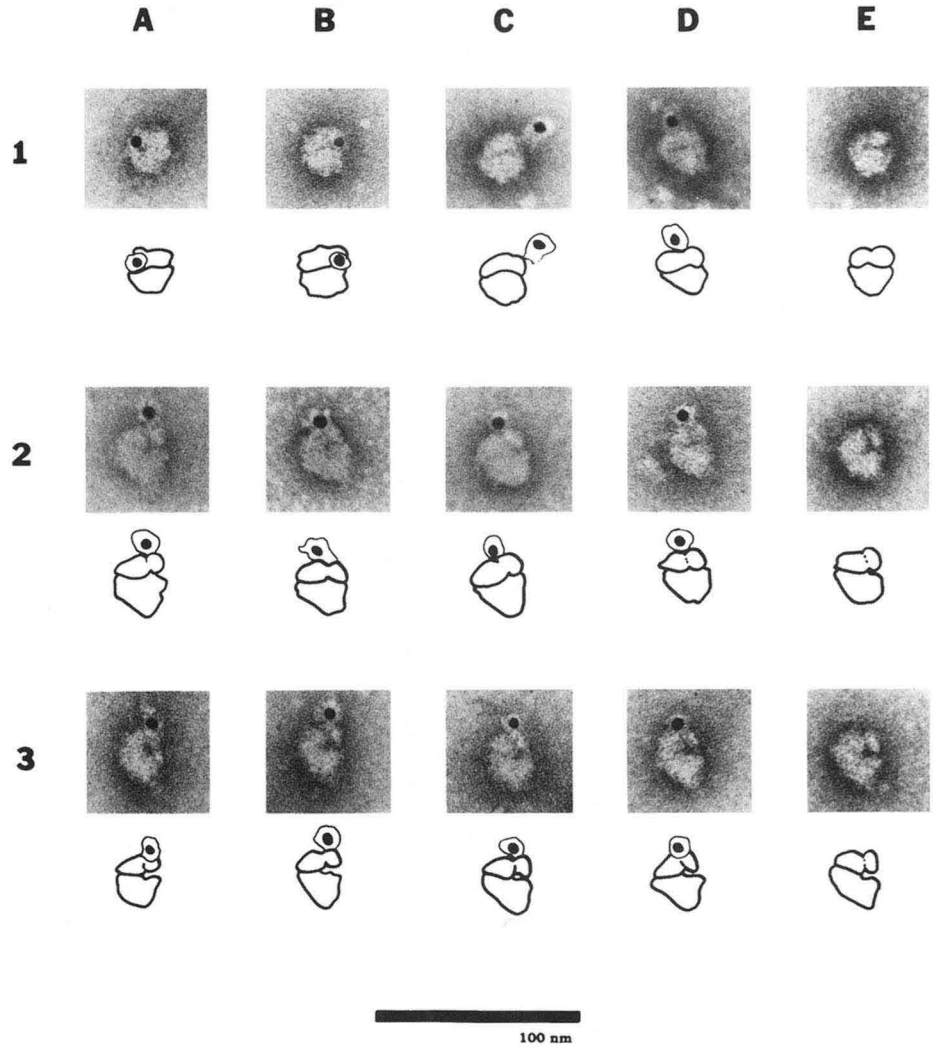


FIG. 7. **Identification of U2 snRNP and localization of the 5′ segment of U2 snRNA in the *A*-complex.** The *A*-complex was hybridized with 5′-biotinyl-cOmeRNA-U2A, reacted with streptavidin-gold (5 nm), and visualized in electron micrographs. *Rows 1–3* show slightly different orientations of the *A*-complex-oligonucleotide-gold complex. *Panel A1* shows a mirror image view of the other particles in the row. *Column E* shows similar images of free *A*-complex.

lies atop the U1 snRNP, with the line of stain separating the components. Rotation about the horizontal axis through the interface results in more or less exposure of the upper component, and partial separation or "breathing" of the components appears to sometimes allow greater penetration of stain between the subparticles. Contact between the two components is most obvious in the body segments that contain the core proteins, and the amount of apparent interaction between U1 and U2 snRNPs is greater than predicted by many studies; in fact it has been suggested that U1 dissociates from the pre-mRNA when U2 binds (47, 54–57). SAPs, if present, do not appear to significantly alter the profiles of the individual snRNPs. Again, they may play a role in the interactions that maintain the structure we see.

Labeling of the U2 snRNP with 5′-biotinyl-cOmeRNA-U2A and streptavidin-gold clearly identifies the upper component of the *A*-complex as U2 snRNP (Fig. 7). The gold label is attached to a protein which is further bound to the modified oligonucleotide which is hybridized with the snRNA; there is certainly some flexibility in this chain of components, and it is apparent in the visualization of gold beside or on top of the head portion of the U2 snRNP. The site of the 5′-segment of U2 snRNA in the *A*-complex, although not placed at a high level of resolution, is very clearly in the head/neck region of the U2 snRNP. A similar localization for the 5′-end of the U2 snRNA has been postulated from studies in which isolated 17 S U2 snRNPs were exposed to high salt concentrations or treated with RNase H and a variant of cDNA-U2A (45), converting the 17 S dumbell to a less symmetric, nearly globular 12 S particle that still contains the core proteins. The 5′ segment of the snRNA is also physically close to the pre-mRNA branch point; the biotin marker is at nucleotide 20 of U2 snRNA, and variants of cDNA-U2B which encompass nucleotides 27–44 block binding of U2 snRNP to the branch point sequence (27, 30, 36). Moreover, upon association of the tri-snRNP the 5′ portion of U2 snRNA binds the 3′-end of U6 snRNA and the branch point sequence; these events result in the juxtaposition of the 5′ splice site, the branch point sequence, and the purported catalytic domain of U6 snRNA (6, 47). This indicates that the area marked by the gold label in Fig. 7 is at or near the assembling catalytic center of the spliceosome.

Thus, the *A*-complex isolated by our approach can be functionally defined as a bipartite structure composed of U1 and U2 snRNPs bound to the pre-mRNA, and trapped prior to the replacement of U1 by the tri-snRNP complex (47, 54). The region near the U2 head/neck junction appears to be part of the assembling catalytic center of the spliceosome, while the core proteins appear more likely to be in regions that are involved in stabilization of snRNP-snRNP interactions. Further identification and mapping of the pre-mRNA and the protein and RNA components of each snRNP, using techniques that have been proven in studies of the ribosome (*e.g.* Refs. 49, 58, and 59), should now be straightforward.

*Acknowledgments*—We thank Drs. Eddy DeRobertis, David Meyer, and Sallie Hoch who generously provided antibodies, Dr. Michael Carey

who provided facilities and advice for cell culture and extract preparation, and Dr. Douglas Black who provided us with the adenovirus construct and for useful discussions of these experiments.

REFERENCES

1. Lamm, G. M., and Lamond, A. I. (1993) *Biochim. Biophys. Acta* **1173,** 247–265
2. Moore, M., Query, C., and Sharp, P. (1993) in *The RNA World* (Gesteland, R., and Atkins, J., eds) pp. 303–357, Cold Spring Harbor Laboratory Press, Cold Spring Harbor, NY
3. Newman, A. (1994) *Curr. Opin. Cell Biol.* **6,** 360–367
4. Nilsen, T. (1994) *Cell* **78,** 1–4
5. Steitz, J. (1992) *Science* **257,** 888–889
6. Wise, J. (1993) *Science* **262,** 1978–1979
7. Jamison, S., Crow, A., and Garcia-Blanco, M. (1992) *Mol. Cell. Biol.* **12,** 4279–4287
8. Bindereif, A., and Green, M. R. (1987) *EMBO J.* **6,** 2415–2424
9. Konarska, M., and Sharp, P. (1987) *Cell* **49,** 763–774
10. Zillman, M., Zapp, M., and Berget, S. (1988) *Mol. Cell Biol.* **8,** 814–821
11. Bennett, M., Michaud, S., Kingston, J., and Reed, R. (1992) *Genes & Dev.* **6,** 1986–2000
12. Gozani, O., Patton, J., and Reed, R. (1994) *EMBO J.* **13,** 3356–3367
13. Michaud, S., and Reed, R. (1991) *Genes & Dev.* **5,** 2534–2546
14. Reed, R., Griffith, J., and Maniatis, T. (1988) *Cell* **53,** 949–961
15. Ruby, S., Goelz, S., Hostomsky, Z., and Abelson, J. (1990) *Methods Enzymol.* **181,** 97–121
16. Ryder, U., Sproat, B., and Lamond, A. (1990) *Nucleic Acids Res.* **18,** 7373–7379
17. Newman, A., and Norman, C. (1992) *Cell* **68,** 743–754
18. Madhani, H., and Guthrie, C. (1992) *Cell* **71,** 803–817
19. Liao, X., Colot, H., Wang, Y., and Rosbash, M. (1992) *Nucleic Acids Res.* **20,** 4237–4245
20. Baserga, S., and Steitz, J. (1993) in *The RNA World* (Gesteland, R., and Atkins, J., eds) pp. 359–381, Cold Spring Harbor Press, Cold Spring Harbor, NY
21. Grabowski, P., and Sharp, P. (1986) *Science* **233,** 1294–1299
22. Fu, X.-D. (1993) *Nature* **365,** 82–85
23. Crispino, J., Blencowe, B., and Sharp, P. (1994) *Science* **265,** 1866–1869
24. Kohtz, J., Jamison, S., Will, C., Zuo, P., Lührmann, R., Garcia-Blanco, M., and Manley, J. (1994) *Nature* **368,** 119–124
25. Clark, M., Goelz, S., and Abelson, J. (1988) *EMBO J.* **7,** 3829–3836
26. Sibbald, M. J., Carlemalm, E., Beer, M., and Sproat, B. (1993) *J. Struct. Biol.* **110,** 111–121
27. Barabino, S., Sproat, B., Ryder, U., Blencowe, B., and Lamond, A. (1989) *EMBO J.* **8,** 4171–4178
28. Barabino, S., Blencowe, B., Ryder, U., Sproat, B., and Lamond, A. (1990) *Cell* **63,** 293–302
29. Blencowe, B., Sproat, B., Ryder, U., Barabino, S., and Lamond, A. (1989) *Cell* **59,** 531–539
30. Lamond, A., Sproat, B., Ryder, U., and Hamm, J. (1989) *Cell* **58,** 383–390
31. Sproat, B., Lamond, A., Beijer, B., Neuner, P., and Ryder, U. (1989) *Nucleic Acids Res.* **17,** 3373–3386
32. Sinha, N. D., Biernat, J., McManus, J., and Koster, H. (1984) *Nucleic Acids Res.* **12,** 4539–4557
33. Lasater, L., Olson, H. M., Cann, P., and Glitz, D. G. (1988) *Biochemistry* **27,** 4687–4695
34. Dignam, J., Lebovitz, R., and Roeder, R. (1983) *Nucleic Acids Res.* **11,** 1475–1489
35. Black, D., and Steitz, J. (1986) *Cell* **46,** 697–704
36. Black, D., Chabot, B., and Steitz, J. (1985) *Cell* **42,** 737–750
37. Solnick, D. (1985) *Cell* **42,** 157–164
38. Krainer, A., Maniatis, T., Ruskin, B., and Green, M. (1984) *Cell* **36,** 993–1005
39. Hortsch, M., Avossa, D., and Meyer, D. (1986) *J. Cell Biol.* **103,** 241–253
40. Billings, P., Allen, R., Jensen, F., and Hoch, S. (1982) *J. Immunol.* **128,** 1176–1180
41. Matter, L., Schoffer, K., Wilhelm, J., Nyffenegger, T., Parisot, R., and DeRobertis, E. (1982) *Arthr. Rheum.* **25,** 1278–1283
42. Lake, J. A. (1976) *J. Mol. Biol.* **105,** 131–159
43. Hall, K. B., and Konarska, M. (1992) *Proc. Natl. Acad. Sci. U. S. A.* **89,** 10969–10973
44. Black, D., and Pinto, A. (1989) *Mol. Cell Biol.* **9,** 3350–3359
45. Behrens, S., Tyc, K., Kastner, B., Reichelt, J., and Lührmann, R. (1993) *Mol. Cell. Biol.* **13,** 307–319
46. Champion-Arnaud, P., and Reed, R. (1994) *Genes & Dev.* **8,** 1974–1983
47. Staknis, D., and Reed, R. (1994) *Mol. Cell Biol.* **14,** 2994–3005
48. Lührmann, R., Kastner, B., and Bach, M. (1990) *Biochim. Biophys. Acta* **1087,** 265–292
49. Olson, H. M., Lasater, L. S., Cann, P. A., and Glitz, D. G. (1988) *J. Biol. Chem.* **263,** 15196–15204
50. Brosi, R., Groning, K., Behrens, S., Lührmann, R., and Kramer, A. (1993) *Science* **262,** 102–105
51. Fabrizio, P., Esser, S., Kastner, B., and Lührmann, R. (1994) *Science* **264,** 261–265
52. Kastner, B., and Lührmann, R. (1989) *EMBO J.* **8,** 277–286
53. Kastner, B., Kornstadt, U., Bach, M., and Lührmann, R. (1992) *J. Cell Biol.* **116,** 839–849
54. Konforti, B., Koziolkiewicz, M., and Konarska, M. (1993) *Cell* **75,** 863–873
55. Konforti, B., and Konarska, M. (1994) *Genes & Dev.* **8,** 1962–1973
56. Konarska, M., and Sharp, P. (1986) *Cell* **46,** 845–855
57. Grabowski, P. (1990) *Methods Enzymol.* **184,** 319–327
58. Olson, H. M., Nag, B., Etchison, J. R., Traut, R. R., and Glitz, D. G. (1991) *J. Biol. Chem.* **266,** 1896–1902
59. Montesano-Roditis, L., and Glitz, D. G. (1994) *J. Biol. Chem.* **269,** 6458–6470